UNIVERSITY OF LEEDS

This is a repository copy of *A novel interaction between the 5' untranslated region of the Chikungunya virus genome and Musashi RNA binding protein is essential for efficient virus genome replication.*.

White Rose Research Online URL for this paper:
https://eprints.whiterose.ac.uk/197901/

Version: Preprint

White Rose
university consortium
Universities of Leeds, Sheffield & York

eprints@whiterose.ac.uk
https://eprints.whiterose.ac.uk/

1 **A novel interaction between the 5' untranslated region of the**

2 **Chikungunya virus genome and Musashi RNA binding protein**

3 **is essential for efficient virus genome replication**

4

5 **Authors: Kaiwen Sun, Marietta Müller, Catriona Macfarlane, Mark Harris and**

6 **Andrew Tuplin***

7

8 **Correspondence: a.k.tuplin@leeds.ac.uk**

9

10 **Affiliations: Astbury Centre for Structural Molecular Biology and School of**

11 **Molecular and Cellular Biology, Faculty of Biological Sciences, University of Leeds,**

12 **Leeds LS2 9JT, UK.**

13

14

15

16

17

18

19

20

21

22

23

Abstract

Chikungunya virus (CHIKV) is a re-emerging, pathogenic alphavirus that is transmitted to humans by *Aedes spp*. mosquitoes—causing fever and debilitating joint pain, with frequent long-term health implications and high morbidity. The CHIKV lifecycle is poorly understood and specific antiviral therapeutics or vaccines are lacking. In the current study, we identify host cell Musashi RNA binding protein-2 (MSI-2) as a proviral factor. MSI-2 depletion and small molecule inhibition assays, demonstrated that MSI-2 is required for efficient CHIKV genome. Depletion of both MSI-2 and MSI-1 homologues resulted in a synergistic increase in CHIKV inhibition, suggesting redundancy in their proviral function. EMSA competition studies demonstrated that MSI-2 interacts specifically with an RNA binding motif within the 5' untranslated region (5'UTR) of CHIKV and reverse genetic analysis showed that mutation of the binding motif inhibited genome replication and blocked rescue of mutant virus. For the first time, this study identifies the proviral role of MSI RNA binding proteins in the replication of the CHIKV genome, providing important new insight into mechanisms controlling replication of this significant human pathogen and offers the potential of a new therapeutic target.

INTRODUCTION

46 Chikungunya virus (CHIKV) is an alphavirus of the *Togaviridae* family that is

47 transmitted by *Aedes spp.* mosquitos. CHIKV is closely related to other alphaviruses

48 such as Semliki Forest virus (SFV), Venezuelan equine encephalitis virus (VEEV), and

49 sindbis virus (SINV) [1, 2]. CHIKV was first identified in Tanzania in 1952 and

50 symptoms typically include acute febrile symptoms, myalgia, rash and severe

51 arthralgic joint pain, which may persist for months or years [3]. CHIKV recently

52 caused epidemic outbreaks across regions in Asia, Africa, the Americas, the Middle

53 East and Southern Europe [3]. To date, three phylogenetically distinct lineages of

54 CHIKV have been identified, namely the West African, Asian and the East Central

55 Southern African (ECSA) lineages [4]. There remains no clinically approved vaccine or

56 specific antiviral therapy, due in part to a lack of detailed understanding of the CHIKV

57 replication cycle and its interaction with host cell factors.

58

59 CHIKV is an enveloped, positive-sense single-stranded RNA virus with a ~11.8 Kb

60 genome, containing two open reading frames (ORFs) flanked by 5' and 3'

61 untranslated regions (UTRs) (**Fig. 1A**). The 5' UTR is ~ 76 nts in length and is capped

62 by 5' type-0 N-7-methylguanosine. The upstream ORF (ORF-1) encodes the viral non-

63 structural proteins 1-4 (nsP1-4), which are translated directly from the genomic RNA

64 as a single polyprotein that is subsequently proteolytically cleaved into the four

65 mature proteins [5]. Through analogy with other alphaviruses, proteolytic cleavage

66 of nsP1-4 in *cis* by nsP2 releases nsP4 which, as the RNA-dependent RNA polymerase

67 (RdRp), initiates synthesis of the minus-strand intermediate RNA. Subsequent

68 proteolytic cleavage of the remaining nsP123 polyprotein initiates replication of

69 genomic and sub-genomic (29S) RNAs from the minus-strand template [6]. The

70   downstream ORF (ORF-2) encodes the structural polyprotein that is processed into

71   the capsid protein, E3, E2, 6K, and E1.

72

73   While negative strand replication is initiated at the 3' end of the virus genome, as

74   with many positive single stranded RNA viruses, regulatory elements and

75   interactions within the 5' end of the CHIKV genome are required for its initiation and

76   regulation [7]. We and others have previously demonstrated that such regulatory

77   elements include functional RNA secondary structures and higher order interactions

78   within the CHIKV 5'UTR and adjacent upstream region of ORF-1 (**Fig. 1B**). It has been

79   speculated that these RNA elements may regulate template specificity and temporal

80   control of switching, between CHIKV translation and genome replication [8, 9].

81

82   In a previously published study, we demonstrated by SHAPE mapping and reverse

83   genetic analysis that the CHIKV 5'UTR and adjacent ORF-1 coding region is highly

84   structured [9]. However, the study also highlighted a single-stranded region (nts 63-

85   69) that exhibited very high SHAPE reactivity (associated with unpaired bases) and

86   was located immediately between two RNA structures, that we demonstrated were

87   essential for initiation of CHIKV genome replication **(Fig 1B)**. Interestingly, *in silico*

88   analysis noted that nts [63]AUUAAU[68] were closely homologous to the Musashi RNA

89   binding protein (MSI) consensus binding sequence ((G/A)U_{1-3}AGU). MSI are highly

90   conserved RNA binding proteins, containing two highly conserved tandem RNA

91   recognition motifs (RNP-1 and RNP-2), that interact with RNA via the same

92   consensus binding motif. Two MSI homologues have been identified, MSI-1 and MSI-

93   2, that share over 90% homology in their RNA-binding domains and a high degree of

94   functional complementarity and redundancy [10, 11]. MSI have key roles in post-

95   transcriptional regulation of genes involved in development, cell cycle regulation and

96   maintenance of adult neural stem/progenitor cells [12]. A recent study

97   demonstrated that MSI-1 promotes Zika Virus (ZIKV) genome replication in neurons,

98   via interaction with the consensus binding site within the viral 3'UTR [13].

99

100   In the current study, we demonstrate through a range of infectious clone and sub-

101   genomic replicon reporter assays that MSI-2 is required for efficient CHIKV genome

102   replication. A small molecule inhibitor of MSI-1 and MSI-2 reduced infectious virus

103   production by inhibition of CHIKV genome replication. Similarly, MSI-2 silencing by

104   shRNA and siRNA inhibited both infectious virus production and genome replication,

105   while co-silencing of both MSI-2 and MSI-1 resulted in a synergistic increase in

106   inhibition of CHIKV replication. Reverse genetic analysis, in which the putative MSI

107   binding site within the CHIKV 5'UTR was mutated, completely prevented rescue of

108   mutant virus and inhibited CHIKV genome replication. Biochemical MSI-2 binding

109   analysis by competition electromobility shift assay (EMSA) demonstrated that

110   recombinantly expressed MSI-2 specifically interacts with the 5' region of the CHIKV

111   genome and that this interaction is inhibited by mutation of the putative MSI 5'UTR

112   binding site. These findings demonstrate for the first time that interaction between

113   MSI and a binding site within the 5'UTR are required for replication of the CHIKV

114   genome.

115

116   **Materials and Methods**

117

118   **Cell culture**

119   Human Rhabdomyosarcoma (RD), Human hepatoma (Huh7), Baby Hamster Kidney

120   (BHK) and Human Embryonic Kidney (HEK) 293 were grown in Dulbecco's modified

121   eagle's medium (DMEM; Sigma) containing 10% fetal bovine serum (FBS; PAA), 1x

122   penicillin-streptomycin (Sigma), 25mM HEPES in 0.85% NaCl (Lonza) and 1% non-

123   essential amino acids mixture (NEAA; Lonza). Cells were harvested using

124   trypsin/EDTA, seeded at dilutions of 1:3 to 1:10 and maintained at 37°C in 5% CO_2.

125

126   **CHIKV cDNA plasmid**

127   The infectious CHIKV (ICRES), CHIKV Dual-luciferase sub-genomic replicon (CHIKV-

128   SGR) and *trans*-complementation (pCHIKV-nsP1234 and pCHIK-Fluc/Gluc) assay were

129   derived from the CHIKV ESCA strain, isolate LR2006 OPY1 (accession number

130   DQ443544)[14]. In CHIKV-SGR the second ORF was replaced by a firefly luciferase

131   gene and a *Renilla* luciferase gene was fused within nsP3 [15]. The *trans*-

132   complementation assay utilised a CMV codon optimised plasmid to supply the CHIKV

133   replicase in *trans* (pCHIKV-nsP1234) and a Pol II expressed reporter plasmid (pCHIKV-

134   FLuc/GLuc), in which the majority of ORF-1 (downstream of nt 320) was replaced by

135   a firefly luciferase gene and all of ORF-2 by a Gaussia Luciferase gene [16]. Plasmid

136   cDNA was purified using GeneJET Plasmid Maxiprep kits (Thermo Fisher Scientific)

137   according to the manufacturer's instructions.

138   **Virus production**

139   1×10^6 BHK cells were trypsinised and resuspended in 400 µl ice-cold DEPC-PBS. Cells

140   were then electroporated with 1 µg 5'-capped CHIKV ICRES *in vitro* transcribed RNA

141   in a 4 mm electro-cuvette, with a single square wave pulse at 260 V for 25 ms using a

142   Bio-Rad electroporator, before seeding into a T175 flask in 20 ml DMEM. After 24 h,

143   supernatant was aspirated and virus titre measured by plaque assay on BHK cells.

144

145   **CHIKV quantification by plaque assay**

146   BHK cells were seeded at 1×10^5 cells per well in 12-well plates and maintained

147   overnight in 1 ml DMEM. The following day monolayers were washed with PBS,

148   infected with 10-fold serial dilutions of CHIKV transfection supernatant and

149   maintained at 37 °C. 1 hpi monolayers were washed with PBS and covered with a

150   0.8% methylcellulose DMEM P/S overlay. 48 hpi monolayers were fixed and stained

151   (5% paraformaldehyde and 0.25% crystal violet respectively), plaques counted and

152   virus titres expressed in plaque-forming units per ml (PFU/ml).

153

154   **Ro 08-2750 cell viability assay**

155   RD cells were seeded in 96-well plate at 8×10^4 cells/well and maintained for 24 hrs.

156   Monolayers were then treated with increasing doses (0, 0.5, 1, 3, 5, 7, 10, 20 µM) of

157   Ro 08-2750 (TOCRIS) dissolved in DMSO. After 24 hrs media/inhibitor was aspirated

158   and replaced with 20 µl of 5 mg/mL 3-(4,5-dimethylthiazol-2-yl)-2,5-

159   diphenyltetrazolium bromide (MTT) (Sigma) and incubated at 37 °C in 5% CO_2 for 3

160   hrs. After incubation, MTT solution was replaced with 100 µl DMSO and the plate

161   shaken at 60 rpm for 5 min. Absorbance at 570 nm was determined using an Infinite

162   F50 microplate reader (Tecan) and expressed as a percentage of DMSO control cells.

163   5 µM Ro 08-2750 was estimated to be the maximum non-toxic dose in in Huh7 cells

164   and was used for all further assays.

165

166   **Infectious CHIKV Ro 08-2750 inhibition assays**

167   RD cells were seeded in 12-well plates at 1x10^5 cells/well and incubated overnight in

168   the presence of Ro 08-2750. Monolayers were then infected with CHIKV at MOI=0.1

169   and adsorbed to the cells for 1 h at 37°C before aspirating and maintaining in the

170   presence of Ro 08-2750 for 24 hrs. Supernatants was then collected and infectious

171   virus production measured by plaque assay.

172

173   **siRNA depletion of MSI-1 and MSi-2**

174   RD or Huh7 cells were seeded at 1x10^5 cell/well in 12-well plates in antibiotic-free

175   medium. After 24 hrs, cells were washed with PBS and incubated with 1x Opti-MEM

176   + GlutaMAX (Gibco) for 20 min at 37°C/5% CO_2. For each well, 50 pmol MSI-1 (sc-

177   106836; Santa Cruz) and/or MSI-2 siRNA (sc-75834; Santa Cruz) were mixed with 100

178   µl Opti-MEM and incubated at room temperature for 1min. No siRNAs were added

179   to mock samples and 50 pmol of scrambled siRNA (SI03650318; QIAGEN) was used

180   as a negative control. In parallel, 3 µl Lipofectamine RNAiMAX (Invitrogen) was

181   mixed with 100 µl Opti-MEM and incubated at room temperature for 1 min. The

182   siRNA and Lipofectamine RNAiMAX were mixed and incubated at room temperature

183   for 5 min before adding to the cells. After 24 hrs, cells were either lysed to confirm

184   MSI-1 or MSi-2 depletion by western blot or used for subsequent CHIKV infection

185   assays.

186

shRNA depletion of MSI-1 and MSi-2

Human embryonic kidney 293 (HEK 293T) cells were plated in antibiotic-free DMEM

in 6-well plates and maintained until confluency reached ~80%. For each

transfection, in a single tube 300 μL OptiMEM was mixed with 1 μg p8.9 packaging

plasmids, 1 μg envelope plasmid and either 1.5 μg MSI-2 shRNA or scrambled shRNA

(Santa Cruz Biotechnology); in another tube, 300 μL of OptiMEM was mixed with 5

μL lipofectamine 2000 (Invitrogen). Both tubes were gently mixed by flicking,

incubated at room temperature for 5 min, mixed together and incubated for 20 min

at room temperature. The antibiotic-free DMEM was aspirated and the monolayers

washed once with PBS. 800 μL Opti-MEM was added to each well before dropwise

addition of the lentiviral plasmids/shRNA mixture. After maintenance at 37°C for 6

hrs the media was changed to antibiotic-free DMEM. 48 hpt the lentivirus containing

supernatant was harvested and filtered through a 0.45 μm filter.

RD cells were seeded at 1×10^5 cells/well the day prior to transduction. 1 mL of the

lentivirus supernatant and polybrene (MERCK) were added to each well and

incubated for 6 hrs before aspirating and replacing with antibiotic free DMEM. After

72 hrs media was replaced with DMEM containing 2.5 μg/ml puromycin, in which the

cells were then maintained. The efficiency of the shRNA MSI-2 depletion was

confirmed by western blot.

208   **Strand-specific Quantification of CHIKV RNA**

209   Total RNA was extracted from infected cells using TRI Reagent Solution (Applied

210   Biosystems) according to the manufacturer's instructions. Strand-specific RT-qPCR

211   (ssRT-qPCR) was performed as previously described [17]. Briefly, 500 ng of RNA was

212   reverse-transcribed with gene specific primers (Supplementary information 1) using

213   the SCRIPT cDNA Synthesis Kit (Jena Bioscience) according to the manufacturer's

214   protocol. 100 ng of strand-specific cDNA was used as template for the quantitative

215   PCR performed with the qPCRBIO SyGreen Blue Mix Lo-ROX (PCR Biosystems), with

216   gene specific primers amplifying a 94 bp region of the CHIKV nsP1-encoding

217   sequence using the following PCR program: 95°C for 2 mins, 40 x (95°C for 5 sec,

218   60°C for 30 sec), dissociation curve 60°C-95°C as pre-defined by the Mx3005P

219   thermal cycler (Agilent technologies). *In vitro* transcribed CHIKV ICRES RNA was

220   reverse transcribed and a cDNA dilution series employed as a standard to quantify

221   copy numbers in the respective samples.

222

223   *In vitro* **RNA transcription**

224   To generate CHIKV-SGR and infectious CHIKV RNA, 2 µg of cDNA was linearised with

225   Not-I HF and used as a template for transcription of 5' [m7G(5')ppp(5')G] capped

226   (m7G capped) RNA, using an SP6 mMessage mMachine kit, according to the

227   manufacturer's instructions (Life Technologies). Uncapped CHIKV 1–337 RNA, used

228   1 µg of CHIKV 1–337 PCR DNA as a template for *in vitro* transcription using the SP6-

229   Scribe™ standard RNA IVT kit, according to the manufacturer's instructions (Lucigen).

230   In all cases, following DNase I treatment, RNA was purified by LiCl precipitation and

231   analysed by denaturing agarose gel electrophoresis.

232

233   **CHIKV Sub-genomic replicon assays**

234   For analysis of Ro 08-2750 inhibition, RD cells were seeded in 24 well plates at

235   5×10^4 cells per well and maintained overnight in the presence of Ro 08-2750.

236   Monolayers were washed once in PBS before addition of 400 µl opti-Mem reduced-

237   serum media and 100 µl transfection media. Transfection media was prepared

238   according to the manufacturer's instructions, using 1 µl Lipofectamine 2000

239   (Invitrogen), 250 ng of CHIKV-SGR RNA and appropriate concentrations of Ro 08-

240   2750, before being made up to 100 µl using opti-Mem. Monolayers were maintained

241   for 6 hpt before the media was aspirated and replaced with complete DMEM/Ro 08-

242   2750. At 8 and 24 hpt monolayers were lysed with 100 µl 1 x passive lysis buffer

243   according to the manufacturer's instructions (Promega), stored at −80 °C and

244   analysed using Dual-luciferase substrate (Promega) in a FLUOstar Optima

245   luminometer (BMG labTech). For shRNA MSI-2 depleted cell lines the same method

246   was followed, with the exclusion of Ro 08-2750.

247

248   ***Trans*-complementation Assay**

249   The *trans*-complementation assay was performed as previously described [18].

250   Briefly, for analysis of Ro 08-2750 inhibition, RD cells were seeded in 12 well plates at

251   5×10^4 cells per well and maintained overnight in the presence of Ro 08-2750.

252   Monolayers were then co-transfected with 1 µg each of the pCHIKV-nsP1234 and

253   pCHIKV-FLuc/GLuc using Lipofectamine 2000, as described previously, and assayed

254   at 8 and 24 hpt. For shRNA MSI-2 depleted cell lines the same method was followed,

255   with the exclusion of Ro 08-2750.

256

257   **Expression and purification of recombinant MSI-2 RNA binding domains**

258   The MSI-2 RNA binding domain expressing plasmid pET-22HT-MSI-2 (amino acid 8-

259   193) was a kind gift from Prof S. Ryder (Addgene plasmid # 60356;

260   http://n2t.net/addgene:60356; RRID: Addgene_60356) [19]. The plasmid was

261   transformed into BL21 (DE3) competent cells following the manufacturer's protocol

262   (NEB), a single colony was inoculated into 10 mL LB ampicillin (10 mg/ml) and

263   incubated overnight at 37°C before inoculating 1000 ml 1 LB (ampicillin (10 mg/ml)

264   and adding 100 µM Isopropyl β-D-1-thiogalactopyranoside (IPTG; Thermo Fisher

265   Scientific) when the optical density reached 0.8. The culture was then incubated

266   overnight at 18°C in an orbital shaker before centrifugation to pellet the bacteria.

267   The pellet was resuspended in lysis buffer (20U/mL DNase I, 0.6U/mL RNase A,

268   1mg/mL lysozyme and 1x protease inhibitor) and lysed on ice for 30 min . Following

269   sonication, the suspension was centrifuged twice at 2000 xg for 1 hour at 4°C. The

270   was filtered through a 0.45 µm filter and His-MSI-2 was purified with HisTrap^{TM} FF

271   column (Cytiva) using the Econo Gradient Pump (BIORAD) according to the

272   manufacturer's protocol and overnight dialysis. The purified protein was quantified

273   and the purity and identity assayed by Coomassie SDS-PAGE and western blot

274   (Supplementary data 2).

275

276   After desalting using PD-10 desalting columns (Cytiva), His-MSI-2 protein was further

277   purified by ion exchange chromatography. Following the manufacturer's

278   instructions, the column was equilibrated with wash buffer (50 mM MES, 10 mM

279   NaCl, pH 5.6, degassed) and the protein eluted in the same buffer. Ion exchange

280   chromatography was performed using HiTrap SP HP cation exchange

281   chromatography column (Cytiva) following the manufacturer's instructions and

282   eluted in degassed 50mM MES, 1M NaCl, pH 5.6. The eluted protein fractions were

283   analysed by Coomassie SDS-PAGE and western blot (Supplementary data 2).

284

285   **^{32}P RNA end labelling**

286   *In vitro* transcribed CHIKV RNA (nt's 1-337) was 5' dephosphorylated using Quick CIP

287   according to the manufacturer's instructions (NEB) before purification using an RNA

288   Clean & Concentrator column (Zymo Research). 20 pmoles of dephosphorylated RNA

289   was combined with 2 µl 10 x T4 Polynucleotide Kinase buffer (NEB), 3 µl ATP(γ-^{32}P)

290   10 mCi/ml, 1 µl T4 Polynucleotide Kinase (NEB) and nuclease free H_2O to a final

291   volume of 20 µl, incubated at 37 °C for 60 min, 65 °C for 20 min, purified using an

292   RNA Clean & Concentrator Kit (Zymo Research) and resuspended in RNase-free H_2O.

293

294   **Electromobility shift assay (EMSA)**

295   RNA was incubated at 95°C for 2 min and on ice for 2 min before 3.3 x RNA folding

296   buffer (100 mM HEPES pH 8.0, 100 mM NaCl and 10 mM MgCl2) and RNasin Plus

297   RNase Inhibitor (Promega) was added to a final volume of 10 µl and incubated for

298   20 min at 37°C. MSI-2 protein was combined with 3.3 x RNA folding buffer, 0.5 x TE,

299   100% glycerol, RNasin Plus RNase Inhibitor (Promega) and 5 µg yeast tRNA as non-

300   specific competitor and incubated at 37°C for 2 min before adding to the RNA

301   mixture and further incubation at 37°C for 15 min. Finally, samples were analysed by

302   native PAGE gel electrophoresis at 135 V for ~2 h. The gel was fixed for 30 min and

303   dried with gel dryer (BIORAD), exposed onto Hyperfilm™ ECL™ (Merck) and

304   visualised using a Xograph Film Processor. Band shifts were quantified by

305   densitometry, as a percentage of band density normalised to the total lane density,

306   relative to control lanes.

307

308   **Assessment of MSI-1, MSI-2 and CHIKV protein expression by western blot**

309   Following infection and incubation, monolayers were lysed in IP lysis buffer

310   (Promega) and incubated at room temperature for 30 min. Protein concentration

311   was quantified using a Pierce™ BCA Protein Assay Kit (Thermo scientific) according to

312   the manufacturer's instructions. Equal amounts of protein lysate were analysed by

313   SDS-PAGE. Protein was transferred onto an Immobilon-FL PVFD transfer membrane

314   (MERCK) using a TE77X semi-dry transfer (Hoefer) at 15 V for 60 min. Membranes

315   were blocked using diluted Odyssey® Blocking Buffer in PBS (LI-COR) for 30 min and

316   probed with primary antibodies against β-actin (1:10,000, mouse monoclonal, Sigma-

317   Aldrich A1978), MSI-2 (1:1000 rabbit monoclonal, Abcam ab76148) and MSI-1

318   (1:5000, Abcam ab21628) in diluted Odyssey® Blocking Buffer in PBS (LI-COR)

319   overnight at 4 °C. After overnight incubation, primary antibody was removed and

320   membranes washed 3 times using PBS. Membranes were stained with secondary

321   antibodies (IRDye® 800CW Donkey anti-Mouse; IRDye® 680LT Donkey anti-Rabbit; Li-

322   Cor) for 1 h at room temperature, washed 3 times using 1 x PBS, dried and then

323   imaged using an Odyssey® Fc Imaging System (Li-Cor).

324

325   ***Statistical analysis***

326   Statistical analysis was carried out using one-way ANOVA and Dunnett's multiple

327   comparisons test on GraphPad Prism version 8.4.0. P values of ≤0.05 (*), ≤0.01 (**),

328   ≤0.001 (***) were used to represent degrees of significance between each drug

329   treatment/silencing/mutant to wild-type assay.

330

331   **RESULTS**

332

333   **Ro inhibited replication of CHIKV infectious virus and sub-genomic replicon:**

334   In order to investigate the potential role of MSI on CHIKV replication, we first

335   assessed the effect of a well-characterised MSI small molecule inhibitor, Ro 08-2750

336   (Ro), on CHIKV productive replication in RD cells using both CHIKV infectious virus

337   and a sub-genomic replicon (SGR) assay (Fig 2A). A number of studies have

338   demonstrated that Ro interacts with the MSI RNA binding domains and acts as a

339   competitive inhibitor for its RNA binding activity and subsequent MSI functions

340   within the cell [20, 21] [22]. In the current study Ro was used at a maximum non-

341   toxic dose as determined by MTT assay (Supplementary data 3).

342

343   The effect of Ro on productive CHIKV infection was measured at 8 and 24 hpi and it

344   was observed that pre-treatment and incubation in the presence Ro significantly

345   inhibited infectious CHIKV replication by ~10-fold, relative to DMSO treated negative

346   controls (Fig. 2B). In order to investigate the effect of Ro on specific stages of CHIKV

347   replication we used an SGR construct, in which ORF-2 was replaced by a firefly

348   luciferase (FLuc) gene and a *Renilla* luciferase (Rluc) gene was fused in-frame with

349   ORF-1 nsP3 (Fig 2A)[9]. The SGR assay enabled us to measure the effect of Ro on

350   CHIKV genome replication and translation, in isolation of other stages of virus

351   infection, such as entry or egress. SGR ORF-1 and ORF-2 expression was significantly

352   inhibited at both 8 and 24 hpt, relative to DMSO treated negative controls, indicating

353   that Ro was inhibiting CHIKV replication at the level of virus genome replication or

354   translation (Fig 2C). ORF-1 is translated from full-length genomic transcripts and ORF-

355   2 from 18S sub-genomic transcripts. The observed inhibition of both ORF-1 and ORF-

356   2 expression was consistent with Ro acting at a stage of the replication cycle common

357   to expression of both ORFs.

358

359   **Ro inhibited CHIKV *trans*-complementation assay:**

360   Inhibition of SGR replication demonstrated that Ro was inhibiting CHIKV replication

361   at the level of virus genome replication or translation. In order to dissect this further,

362   we utilised a *trans*-complementation assay, that enabled the measurement of CHIKV

363   genome replication in isolation of virus translation (Fig 3A)[23]. The *trans*-

364   complementation system utilised a codon-optimised CHIKV replicase-expressing

365   plasmid (pCHIKV-nsP1234), which expresses the virus nsPs from a CMV promoter.

366   The expressed nsPs replicate a CHIKV reporter construct (pCHIKV-FLuc/GLuc), in

367   which the majority of ORF-1 is replaced by an FLuc gene and ORF-2 by the Gaussia

368   luciferase (GLuc) gene. The effect of Ro on pCHIKV-FLuc/GLuc expression was

369 measured at 8 and 24 hpt in cells pre-treated with and maintained in the presence of

370 Ro. Both ORF-1 and ORF-2 expression was observed to be significantly inhibited

371 relative to the DMSO treated negative controls, indicating that Ro was inhibiting

372 CHIKV replication specifically at the level of virus genome replication.

373

374 **MSI-2 shRNA silencing inhibits infectious CHIKV replication:**

375 In order to confirm that Ro induced inhibition of CHIKV genome replication was due

376 to specific inhibition of MSI, rather than an unrecognised off target effect of Ro, we

377 next investigated CHIKV replication following shRNA silencing of MSI expression.

378 Analysis of RD cell total protein extract by western blot, demonstrated that MSI-2

379 was strongly expressed in RD cells while MSI-1 was expressed at a very low level

380 (Supplementary data 4). Consequently, we initially investigated the effect of specific

381 MSI-2 shRNA silencing on CHIKV replication. RD cells were transduced with lentiviral

382 vectors encoding shRNA against human MSI-2 and successful silencing was

383 confirmed by western blot (Fig 4A). Negative control cells were treated with either

384 transfection reagent only (mock) or non-specific scrambled shRNA. Following

385 infection of MSI-2 depleted and negative control cells, productive CHIKV infection

386 was measured by plaque assay at 8 and 24 hpi (Fig 4B). Strand specific qRT-PCR was

387 also used to measure levels of genomic (positive strand) and replication

388 intermediate (negative strand) CHIKV RNA at both time points (Fig 4 C and D). As

389 observed previously following treatment with Ro, relative to the scrambled shRNA

390 control productive CHIKV replication was significantly inhibited following shRNA MSI-

391 2 silencing (Fig 4B). Similarly, strand specific qRT-PCR demonstrated that both

392 genomic and replication intermediate CHIKV RNA levels were significantly inhibited

393   (Fig 4 C and D). These results are consistent with CHIKV requiring MSI-2 for efficient

394   genome replication.

395

396   **MSI-2 is required for efficient CHIKV genome replication**

397   In order to confirm that MSI-2 silencing had the same effect on CHIKV genome

398   replication as Ro small molecule inhibition, we repeated analysis with the SGR and

399   *trans*-complementation systems, following shRNA silencing of MSI-2. As previously

400   described, MSI-2 shRNA silenced RD cells were transfected with the SGR system and

401   ORF-1 and ORF-2 expression measured by RLuc and FLuc expression at 8 and 24 hpt

402   (Fig 5A and B). Expression of both ORF-1 and ORF-2 was significantly inhibited at

403   both 8 and 24 hpt, consistent with an MSI-2 requirement for CHIKV genome

404   replication or translation. Analysis at the same time points using the *trans*-

405   complementation system, following shRNA MSI-2 silencing and measuring ORF1 and

406   ORF2 expression, confirmed significant inhibition of CHIKV genome replication when

407   measured in isolation of the effects of other stages of the virus replication cycle (Fig

408   5C and D)

409

410   **Both MSI-2 and MSI-1 have a proviral effect on CHIKV genome replication:**

411   While results clearly demonstrated that MSI-2 was required for efficient CHIKV

412   replication, it remained unclear if MSI homologue MSI-1 was also agonistic for CHIKV

413   replication. As previously described, western blot analysis showed that MSI-1 was

414   not highly expressed in RD cells. Consequently, we analysed MSI homologue

415   redundancy in Huh7 human hepatoma cells, in which both MSI-1 and MSI-2

416   homologues are strongly expressed (Supplementary data 4) and are highly

417   permissive for CHIKV replication [24]. Following individual and combined siRNA

418   silencing of MSI-1 and MSI-2 in Huh7 cells (Supplementary data 5), CHIKV replication

419   was assayed by plaque assay and ssRT-qPCR at 8 and 24 hpi (Fig 6A, B and C). As was

420   observed for RD cells, MSI-2 silencing significantly inhibited CHIKV replication,

421   measured by both plaque assay and strand specific ssRT-qPCR. Interestingly, it was

422   observed that MSI-1 silencing in Huh7 cells had a similar significant inhibitory effect

423   and that siRNA co-silencing of both MSI-1 and MSI-2 had a synergistic effect on

424   inhibition of CHIKV replication. In concordance with previous results, siRNA silencing

425   of MSI-2 in RD cells significantly inhibited CHIKV replication, by comparable levels

426   observed following shRNA silencing and inhibition by Ro. Consistent with low MSI-1

427   expression in RD cells, siRNA co-silencing of both MSI-1 and MSI-2 did not

428   significantly increase levels of CHIKV inhibition (Fig. 6D, E and F).

429

430   **MSI-2 binds specifically to the predicted $_{63}$AUUAAU$_{68}$ 5'UTR MSI binding site in the**

431   **CHIKV 5'UTR**

432   Following confirmation that MSI-2 RNA binding protein is required for efficient CHIKV

433   genome replication, we next used native EMSA to biochemically investigate the

434   potential for a direct interaction between the RNA binding domains of MSI-2 and

435   nucleotides $_{63}$AUUAAU$_{68}$ within the virus 5'UTR, which had close sequence homology

436   to the (G/A)U$_{1-3}$AGU MSI consensus nucleotide binding motif [25]. $_{63}$AUUAAU$_{68}$ is

437   located in single-stranded region of the 5' UTR, 9 nts upstream of the AUG start

438   codon and between two RNA structures that are essential for CHIKV genome

439   replication (Fig. 1B)[9]. The first 330nts of the CHIKV genome (RNA-330),

440   representing the 5'UTR and adjacent upstream region of ORF1, was *in vitro*

441   transcribed, 5' end radiolabelled with ATP-[γ-32P] and incubated at 37°C - conditions

442   under which correct folding of the functional RNA-330 structure was previously

443   validated [9]. Following incubation with increasing concentrations of recombinantly

444   expressed and purified MSI-2 8-193 in the presence of unlabelled tRNA, reaction

445   products were separated by native PAGE and analysed by autoradiography (Fig 7A).

446   Relative to unbound RNA-330, the presence of MSI-2 8-193 resulted in the

447   retardation of RNA-330 migration during native PAGE, consistent with the formation

448   of an RNA-330/MSI-2 8-193 complex. In order to investigate the specificity of the

449   observed interaction, a fixed molar ratio of RNA-330$^{\gamma\text{-}32P}$ and MSI-2 8-193 was

450   incubated with increasing concentrations of competitor unlabelled RNA-330 (Fig 7B).

451   Increasing concentrations of unlabelled RNA-330 reduced the formation of the RNA-

452   330$^{\gamma\text{-}32P}$/MSI-2 8-193 complex, with a corresponding increase in unbound RNA-330$^{\gamma\text{-}}$

453   ^{32P}.

454

455   In order to further confirm the specificity and location of the interaction the putative

456   MSI-2 binding site $_{63}AUUAAU_{68}$ was mutated to $_{63}CAACUU_{68}$ (henceforth termed

457    $_{63}CAACUU_{68}$-mut). EMSA competition with unlabelled $_{63}CAACUU_{68}$-mut RNA-330 was

458   significantly less efficient at competing for MSI-2 8-193 binding than wild-type CHIKV

459   RNA (Fig 7 C and D). These ESMA results are consistent with an interaction between

460   MSI-2 and the upstream region of the CHIKV genome. The significant inhibition of

461   this interaction in the $_{63}CAACUU_{68}$-mut indicated both that the interaction was

462   specific and that nts $_{63}AUUAAU_{68}$ function as an MSI binding motif.

463

464   **Mutagenesis of 5'UTR $_{63}$AUUAAU$_{68}$ MSI binding site inhibits CHIKV genome**

465   **replication and prevents virus rescue**

466   In order to further investigate the role of the $_{63}$AUUAAU$_{68}$ MSI binding motif in CHIKV

467   replication, we took a reverse genetic approach, in which the

468    $_{63}$AUUAAU$_{68}$>$_{63}$CAACUU$_{68}$ mutations were incorporated into both the *trans*-

469   complementation assay and infectious CHIKV. Similar to previous results following

470   MSI inhibition, expression of both ORF-1 and ORF-2 from the *trans*-complementation

471   system were significantly inhibited in $_{63}$CAACUU$_{68}$-mut relative to the wild type at 8

472   and 24 hpt (Fig 8A and B); indicating that mutation of the putative MSI binding site

473   significantly inhibited CHIKV at the level of virus genome replication. Interestingly,

474   despite repeated attempts, we were not able to rescue infectious CHIKV $_{63}$CAACUU$_{68}$-

475   mut virus, indicating that disruption of the potential MSI binding site completely

476   inhibited infectious CHIKV replication (Fig 8C).

477

478   **DISCUSSION**

479

480   For the first time, in this study we demonstrate that cellular RNA binding protein MSI

481   is required for efficient CHIKV replication. Our data demonstrates that MSI-2

482   interacts directly with the 5' end of the CHIKV genome and is consistent with an

483   interaction at position $_{63}$AUUAAU$_{68}$. A single-stranded region located between two

484   conserved stem-loops and immediately upstream of the AUG start codon (Fig 1) [9].

485   Inhibition of MSI-2 expression by siRNA or shRNA, its RNA-binding activity by Ro and

486   reverse genetic disruption of the CHIKV-5'UTR/MSI-2 interaction, inhibited CHIKV

487   replication at the level of virus genome replication. In further analysis, we

488   demonstrated that depletion of both MSI-1 and MSI-2 homologues resulted in a

489   synergistic increase in the level of CHIKV inhibition, supporting the premise that both

490   MSI homologues have a redundant pro-viral effect on CHIKV replication.

491

492   While depletion of MSI-2 by siRNA and shRNA clearly demonstrated significant

493   inhibition of CHIKV replication, measured by infectious virus production, CHIKV-SGR

494   replication or a *trans*-complementation assay, we did not observe complete

495   inhibition of virus replication. Western blot analysis indicated that we did not

496   achieve complete ablation of MSI-2 expression by either siRNA or shRNA,

497   presumably reducing the level of CHIKV inhibition observed. We demonstrated by

498   western blot that in RD cells MSI-2 is expressed to a high level but the MSI-1

499   homologue is only expressed to a low level. However, given the synergistic effect

500   that we observed when silencing expression of both MSI-2 and MSI-1 in Huh7 cells

501   (in which both are expressed to high levels), the ability of MSI homologues to

502   complement for each other may also have reduced the level of CHIKV inhibition

503   observed. This hypothesis is consistent with reverse genetic results, in which

504   mutation of the $_{63}$AUUAAU$_{68}$ MSI binding site, dramatically inhibited the CHIKV-

505   5'UTR/MSI-2 binding affinity and completely prevented rescue of mutant virus.

506

507   Translation and replication of positive-sense RNA virus genomes, such as those of

508   CHIKV are mutually exclusive processes – with translation initiating at the 5' end of

509   the genome and replication at the 3'. Consequently, it is essential that such viruses

510   have mechanisms for temporal control of both processes. In many such viruses (e.g.

22 | P a g e

511   Hepatitis C virus and Polio virus) control involves dynamic interactions between RNA

512   structures in the virus genome and host/virally expressed protein complexes [7]. The

513   mechanisms and interactions which CHIKV and other alphaviruses use for temporal

514   control of genome translation and replication remain unclear. However, a recent

515   study suggested a crucial role for the cellular helicase DHX9. Matkovic et al,

516   demonstrated that interaction between DHX9 and the 5' end of the virus genome

517   upregulates CHIKV ORF-1 non-structural protein translation, while simultaneously

518   inhibiting replication of its genome [26]. Build-up of nsP2 caused proteosome

519   induced degradation of DHX9, although the detailed mechanism for this remains

520   unclear.

521

522   While, genome replication of positive-sense RNA viruses initiates at the 3' end, it is

523   commonly controlled by promoter elements and interactions with RNA binding

524   proteins at the 5' end. Results described in this and previous studies are consistent

525   with a model in which temporal control of CHIKV ORF-1 translation and genome

526   replication is controlled by a mechanism involving interactions between DHX9, MSI2

527   and the 5' region of the virus genome. However, the dynamics and mechanism by

528   which the opposing roles if MSI-2 and DHX-9 influence CHIKV replication and their

529   interactions with the virus genome remains unclear and is the focus of ongoing

530   studies.

531

532   In summary, using MSI-2 depletion and Ro small molecule inhibitor we demonstrate

533   that MSI-2 RNA binding protein is a critical host factor for efficient CHIKV replication.

534   Inhibition of ORF-1 and ORF-2 signal from the *trans*-complementation assay indicate

535 that MSI-2 is required at the level of CHIKV genome replication. Furthermore, EMSA

536 and reverse genetic results are consistent with a direct interaction between MSI-2

537 and $_{63}$AUUAAU$_{68}$ in the positive genomic strand of the virus 5'UTR, suggesting a role

538 in negative strand synthesis. Results from this study are important both for our

539 understanding of the fundamental interactions essential to replication of this

540 important human pathogen and for future studies towards specific antiviral

541 therapies.

542

Funding

543

544 This work was supported by funding from the MRC to AT (MR/NO1054X/1).

545

Data availability statement

546

547 The data underlying this article will be shared on reasonable request to the

548 corresponding author.

549

REFERENCES

550

551

552 1. Fong, S.W., R.M. Kini, and L.F.P. Ng, *Mosquito Saliva Reshapes Alphavirus*
553 *Infection and Immunopathogenesis.* Journal of Virology, 2018. **92**(12).
554 2. McPherson, R.L., et al., *ADP-ribosylhydrolase activity of Chikungunya virus*
555 *macrodomain is critical for virus replication and virulence.* Proceedings of the
556 National Academy of Sciences of the United States of America, 2017. **114**(7):
557 p. 1666-1671.
558 3. Petitdemange, C., N. Wauquier, and V. Vieillard, *Control of immunopathology*
559 *during chikungunya virus infection.* Journal of Allergy and Clinical

560   Immunology, 2015. **135**(4): p. 846-855.

561   4.   Ng, L.F., *Immunopathology of Chikungunya virus infection: lessons learned*

562   *from patients and animal models.* Annual review of virology, 2017. **4**: p. 413-

563   427.

564   5.   Meshram, C.D., et al., *Multiple Host Factors Interact with the Hypervariable*

565   *Domain of Chikungunya Virus nsP3 and Determine Viral Replication in Cell-*

566   *Specific Mode.* J Virol, 2018. **92**(16).

567   6.   Rupp, J.C., et al., *Alphavirus RNA synthesis and non-structural protein*

568   *functions.* Journal of General Virology, 2015. **96**(9): p. 2483-2500.

569   7.   Tuplin, A., *Diverse roles and interactions of RNA structures during the*

570   *replication of positive-stranded RNA viruses of humans and animals.* J Gen

571   Virol, 2015.

572   8.   Frolov, I., R. HARDY, and C.M. RICE, *Cis-acting RNA elements at the 5′ end*

573   *of Sindbis virus genome RNA regulate minus-and plus-strand RNA synthesis.*

574   Rna, 2001. **7**(11): p. 1638-1651.

575   9.   Kendall, C., et al., *Structural and phenotypic analysis of Chikungunya virus*

576   *RNA replication elements.* Nucleic Acids Res, 2019. **47**(17): p. 9296-9312.

577   10.   Troschel, F.M., et al., *Knockdown of Musashi RNA Binding Proteins*

578   *Decreases Radioresistance but Enhances Cell Motility and Invasion in Triple-*

579   *Negative Breast Cancer.* Int J Mol Sci, 2020. **21**(6).

580   11.   Sutherland, J.M., et al., *RNA binding proteins in spermatogenesis: an in depth*

581   *focus on the Musashi family.* Asian J Androl, 2015. **17**(4): p. 529-36.

582   12.   Horisawa, K., et al., *The Musashi family RNA-binding proteins in stem cells.*

583   Biomol Concepts, 2010. **1**(1): p. 59-66.

584   13.   Chavali, P.L., et al., *Neurodevelopmental protein Musashi-1 interacts with the*

585   *Zika genome and promotes viral replication.* Science, 2017. **357**(6346): p. 83-

586   88.

587   14.   Tsetsarkin, K., et al., *Infectious clones of Chikungunya virus (La Reunion*

588   *isolate) for vector competence studies.* Vector Borne Zoonotic Dis, 2006. **6**(4):

589   p. 325-37.

590   15.   Pohjala, L., et al., *Inhibitors of alphavirus entry and replication identified with*

591   *a stable Chikungunya replicon cell line and virus-based assays.* PloS one,

592   2011. **6**(12): p. e28923.

593   16.   Lello, L.S., et al., *Cross-utilisation of template RNAs by alphavirus replicases.*
594   PLoS Pathog, 2020. **16**(9): p. e1008825.

595   17.   Muller, M., et al., *Chikungunya virus requires cellular chloride channels for*
596   *efficient genome replication.* PLoS Negl Trop Dis, 2019. **13**(9): p. e0007703.

597   18.   Bartholomeeusen, K., et al., *A Chikungunya Virus trans-Replicase System*
598   *Reveals the Importance of Delayed Nonstructural Polyprotein Processing for*
599   *Efficient Replication Complex Formation in Mosquito Cells.* J Virol, 2018.
600   **92**(14).

601   19.   Clingman, C.C., et al., *Allosteric inhibition of a stem cell RNA-binding protein*
602   *by an intermediary metabolite.* Elife, 2014. **3**: p. e02848.

603   20.   Arkin, M.R. and J.A. Wells, *Small-molecule inhibitors of protein–protein*
604   *interactions: progressing towards the dream.* Nature reviews Drug discovery,
605   2004. **3**(4): p. 301-317.

606   21.   Niederhauser, O., et al., *NGF ligand alters NGF signaling via p75NTR and*
607   *TrkA.* Journal of neuroscience research, 2000. **61**(3): p. 263-272.

608   22.   Minuesa, G., et al., *Small-molecule targeting of MUSASHI RNA-binding*
609   *activity in acute myeloid leukemia.* Nature communications, 2019. **10**(1): p. 1-
610   15.

611   23.   Lello, L.S., et al., *Cross-utilisation of template RNAs by alphavirus replicases.*
612   PLoS pathogens, 2020. **16**(9): p. e1008825.

613   24.   Roberts, G.C., et al., *Evaluation of a range of mammalian and mosquito cell*
614   *lines for use in Chikungunya virus research.* Scientific reports, 2017. **7**(1): p.
615   1-13.

616   25.   Zearfoss, N.R., et al., *A conserved three-nucleotide core motif defines Musashi*
617   *RNA binding specificity.* J Biol Chem, 2014. **289**(51): p. 35530-41.

618   26.   Matkovic, R., et al., *The Host DHX9 DExH-Box Helicase Is Recruited to*
619   *Chikungunya Virus Replication Complexes for Optimal Genomic RNA*
620   *Translation.* Journal of Virology, 2019. **93**(4).

621

Figure Legends:

623

Figure 1. A) Schematic representation of CHIKV genome organisation **B)** Schematic

representation of CHIKV RNA structures within the 5'UTR and adjacent ORF-1 region

626   of the CHIKV genome (Kendall et al., 2019). RNA replication elements SL3, SL47,

627   SL88, SL102, SL165, SL194 and SL246 are labelled in black type. The ORF-1 AUG start

628   codon is labelled by a green arrow and the putative MSI binding site by a red oval.

629

630   **Figure 2.** Ro signifyingly inhibits replication of infectious CHIKV and the CHIKV-SGR **A)**

631   Schematic representations of CHIKV infectious clone (top) compared to the sub-

632   genomic replicon (SGR) (bottom) in which a *Renilla* luciferase (RLuc) reporter gene is

633   fused within the nsp3 coding sequence and the structural genes of ORF-2 are

634   replaced by a firefly luciferase (Fluc) reporter gene. Replication is expressed in

635   Relative Light Units [RLU] **B)** Ro significantly inhibits productive CHIKV productive

636   replication relative to DMSO treated negative controls at 8 and 24 hpi. **C** and **D)** Ro

637   08-2750 significantly inhibits CHIKV-SGR replication, measured by both ORF-1 and

638   ORF-2 expression, relative to DMSO treated negative controls at 8 and 24 hpt. N=3,

639   error bars represent standard error from the mean and significance was measured

640   by two-tailed T-test (* = $P < 0.05$, ** = $P < 0.01$, *** = $P < 0.001$).

641

642   **Figure 3.** Ro signifyingly inhibits CHIKV genome replication. **A)** Schematic

643   representation of CHIKV *trans*-complementation assay showing codon optimised

644   pCHIKV-nsP1234 (top) from which the CHIKV nsPs were translated and pCHIK-

645   Fluc/Gluc (bottom) in which ORF-1 was replaced by an Fluc reporter gene, fused to

646   the first 77 nts or CHIKV ORF-1 (N77) down-stream of the authentic CHIKV 5'UTR.

647   ORF-2, flanked by the authentic intragenic (SG) and 3' UTRs, was replaced by a Gluc

648   reporter gene. **B** and **C)** Ro significantly inhibited CHIKV genome replication of the

649   *trans*-complementation assay, measured by both ORF-1 and ORF-2 expression,

650   relative to DMSO treated negative controls at 8 and 24 hpt. N=3, error bars

651   represent standard error from the mean and significance was measured by two-

652   tailed T-test (* = $P < 0.05$, ** = $P < 0.01$, *** = $P < 0.001$).

653

654   **Figure 4.** shRNA suppression of MSI-2 significantly inhibits replication of infectious

655   CHIKV. **A)** Western blot analysis of total cellular protein extracted from Rd cells and

656   compared to negative control scrambled shRNA, demonstrated consistent shRNA

657   knockdown of MSI-2 over 3 serial passages (P1- P3). MSI-2 suppression significantly

658   inhibited productive CHIKV replication, relative to scrambled shRNA at 8 and 24 hpi

659   measured by plaque assay **B)** and strand specific qRT-PCR for the the virus genomic

660   **C)** and negative intermediate **D)** strands. N=3, error bars represent standard error

661   from the mean and significance was measured by two-tailed T-test (* = P < 0.05, ** =

662   P < 0.01, *** = P < 0.001).

663

664   **Figure 5.** shRNA suppression of MSI-2 significantly inhibits CHIKV-SGR replication and

665   CHIKV genome replication. **A** and **B)** shRNA suppression of MSI-2 significantly

666   inhibited CHIKV-SGR replication, measured by both ORF-1 and ORF-2 expression,

667   relative to scrambled shRNA negative controls at 8 and 24 hpt. **C** and **D)** shRNA

668   suppression of MSI-2 significantly inhibited CHIKV genome replication of the *trans*-

669   complementation assay, measured by both ORF-1 and ORF-2 expression, relative to

670   DMSO treated negative controls at 8 and 24 hpt. N=3, error bars represent standard

671   error from the mean and significance was measured by two-tailed T-test (* = P <

672   0.05, ** = P < 0.01, *** = P < 0.001).

673

674   **Figure 6**. siRNA Depletion of either MSI-1 or MSI-2 significantly inhibited CHIKV

675   replication in Huh7 cells and co-depletion of both MSI-1 and MSI-2 had a synergistic

676   effect on CHIKV inhibition in Huh7 cells. siRNA depletion of MSI-2 significantly

677   inhibited CHIKV replication in RD cells and co-depletion of both MSI-1 and MSI-2 did

678   not increase the level of CHIKV inhibition. siRNA depletion of MSI-1 and MSI-2

679   significantly inhibited CHIKV replication in Huh7 cells relative to scrambled siRNA at 8

680   and 24 hpi measured by plaque assay **A)** and strand specific qRT-PCR for the the virus

681   genomic **B)** and negative intermediate **C)** strands. siRNA depletion of MSI-2 in RD

682   cells significantly inhibited CHIKV replication in relative to scrambled siRNA at 8 and

683   24 hpi measured by plaque assay **D)** and strand specific qRT-PCR for the the virus

684   genomic **E)** and negative intermediate **F)** strands. N=3, error bars represent standard

685   error from the mean and significance was measured by two-tailed T-test (* = P <

686   0.05, ** = P < 0.01, *** = P < 0.001).

687

688　**Figure 7.** Native EMSAs between *in vitro* transcribed ^{32}P 5' radiolabeled CHIKV RNA

689　nts 1-330 (*RNA^{WT}) and recombinantly expressed MSI-2 demonstrated an

690　RNA/protein interaction that was outcompeted by increasing concentrations of

691　equivalent unlabeled (RNA^{WT}) but less efficiently by the same RNA incorporating

692　BSM mutation $_{63}$AUUAAU$_{68}$ >$_{63}$CAACUU$_{68}$ (RNA^{BSM}). **A)** Increasing concentrations of

693　MSI-2 intensified the observed band shift to the larger RNA/Protein complex and

694　decreased the equivalent unbound RNA band. The interaction between a 1:4 ratio of

695　*RNA^{WT}:MSI-2 was competed with increasing concentrations of unlabelled **B)** RNA^{WT}

696　or **C)** RNA^{mut} ($_{63}$CAACUU$_{68}$-mut). **D)** Band shifts in the unlabeled RNA competition

697　EMSAs were quantified by densitometry and expressed as % change in the density of

698　the RNA/Protein complex bands, normalized to the equivalent total lane density, for

699　each competition ratio and compared each time to ratio 1:0. N=3, error bars

700　represent standard error from the mean and significance was measured by two-

701　tailed T-test (* = P < 0.05, ** = P < 0.01, *** = P < 0.001). Grey block triangles

702　indicate increasing concentrations of specific reactants.

703

704　**Figure 8.** Substitutions within the predicted MSI binding site ($_{63}$CAACUU$_{68}$-mut)

705　prevented rescue of BSM-mutant virus and significantly inhibited CHIKV genome

706　replication. **A** and **B)** Mutation of the MSI binding site significantly inhibited CHIKV

707　genome replication of the *trans*-complementation assay, measured by both ORF-1

708　and ORF-2 expression, relative to wild-type positive controls at 8 and 24 hpt. **C)**

709　Mutation of the predicted MSI binding site prevented rescue of BSM-mutant CHIKV

710　following transfection of capped *in vitro* transcribed RNA into BHK cells. Released

711　virus was measured by plaque assay of supernatant 24 hpt and compared to positive

712　control wild-type infectious CHIKV *in vitro* transcribed RNA, which was transfected

713　and analysed in parallel. N=3, error bars represent standard error from the mean and

714　significance was measured by two-tailed T-test (* = P < 0.05, ** = P < 0.01, *** = P <

715　0.001).
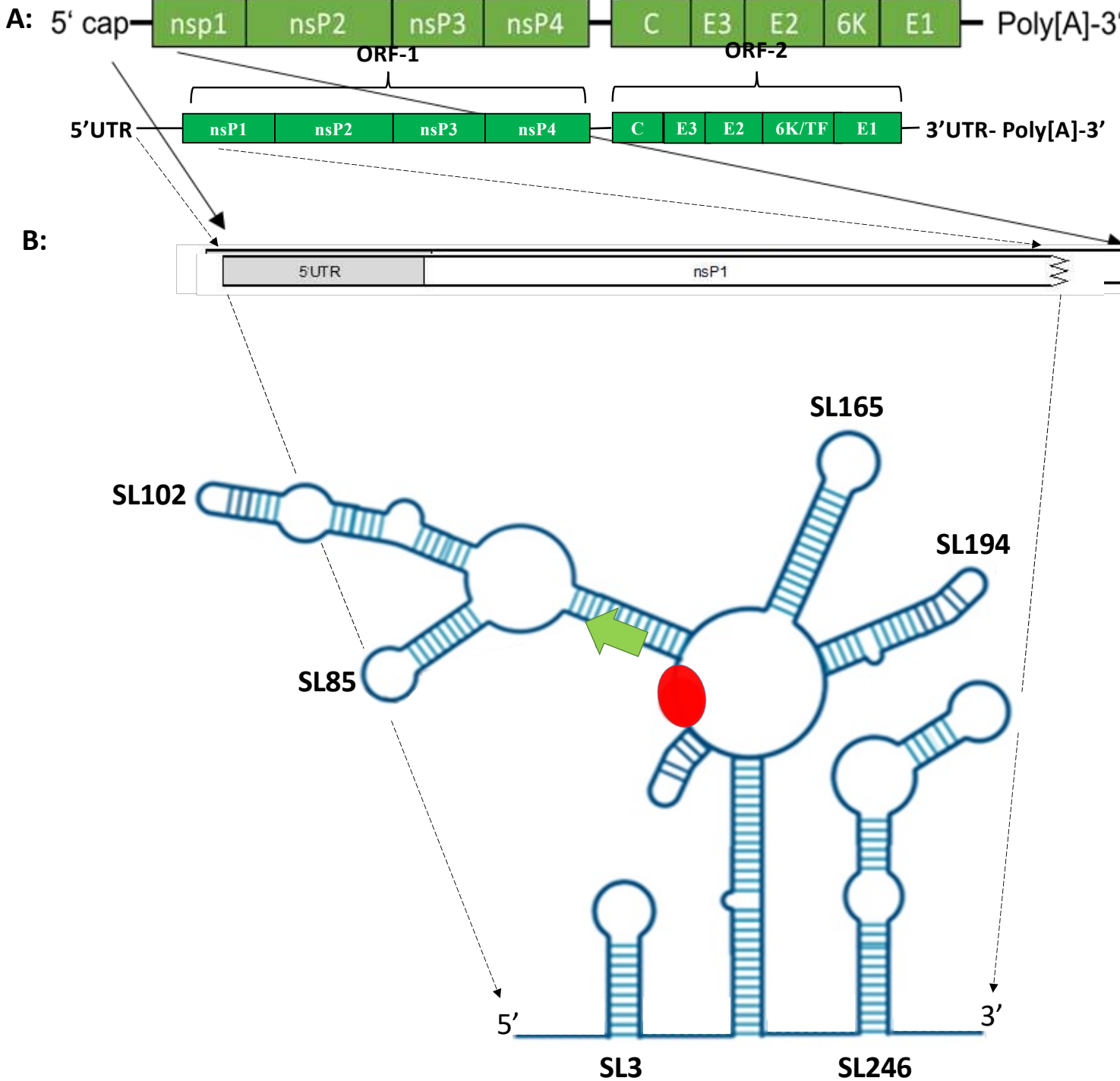
Figure 1. A) Schematic representation of CHIKV genome organisation **B)** Schematic representation of CHIKV RNA structures within the 5'UTR and adjacent ORF-1 region of the CHIKV genome (Kendall et al., 2019). RNA replication elements SL3, SL47, SL88, SL102, SL165, SL194 and SL246 are labelled in black type. The ORF-1 AUG start codon is labelled by a green arrow and the putative MSI binding site by a red oval
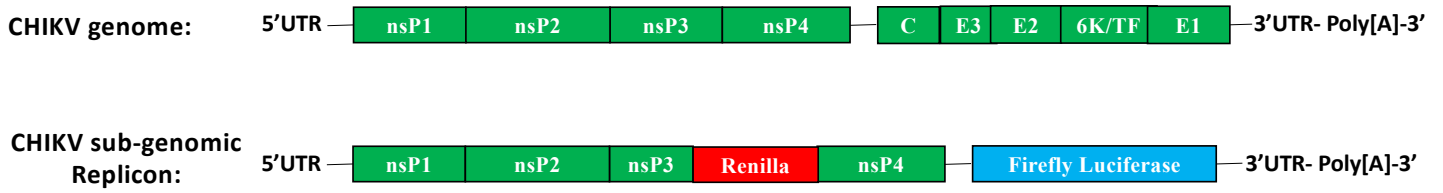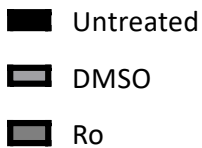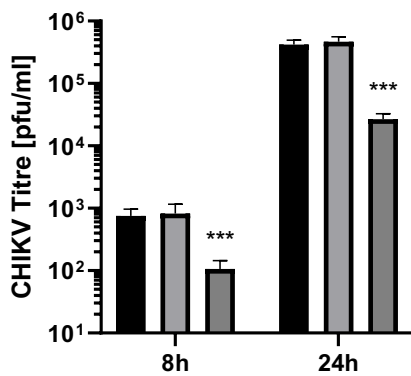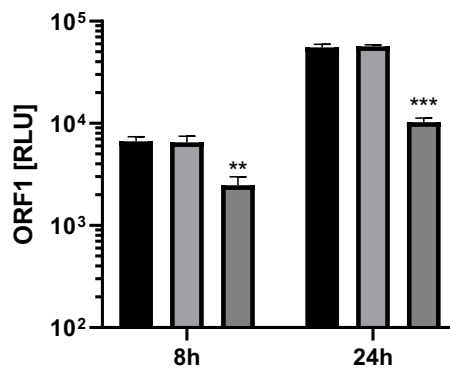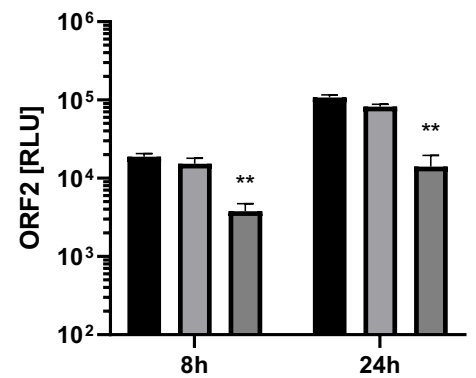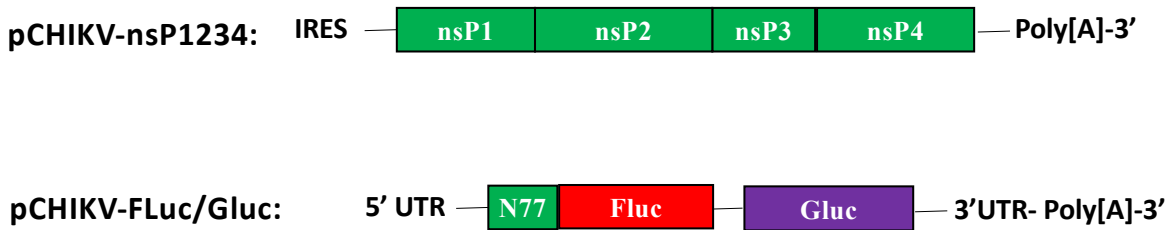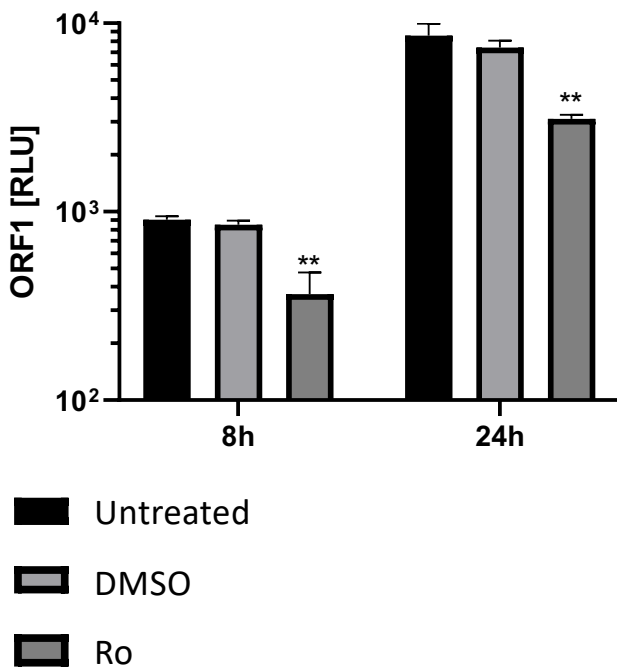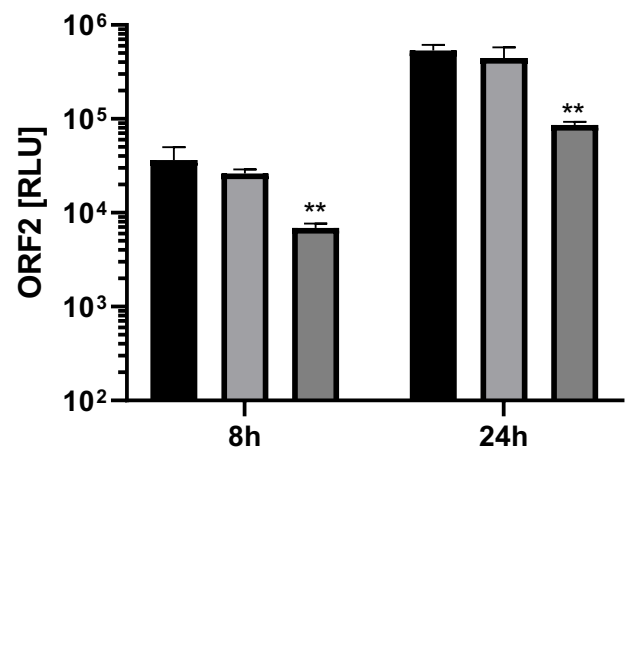
Figure 2. Ro signifyingly inhibits replication of infectious CHIKV and the CHIKV-SGR A) Schematic representations of CHIKV infectious clone (top) compared to the sub-genomic replicon (SGR) (bottom) in which a *Renilla* luciferase (RLuc) reporter gene is fused within the nsp3 coding sequence and the structural genes of ORF-2 are replaced by a firefly luciferase (Fluc) reporter gene. Replication is expressed in Relative Light Units [RLU] **B)** Ro significantly inhibits productive CHIKV productive replication relative to DMSO treated negative controls at 8 and 24 hpi. **C and D)** Ro 08-2750 significantly inhibits CHIKV-SGR replication, measured by both ORF-1 and ORF-2 expression, relative to DMSO treated negative controls at 8 and 24 hpt. N=3, error bars represent standard error from the mean and significance was measured by two-tailed T-test (* = P < 0.05, ** = P < 0.01, *** = P < 0.001).

Figure 3. Ro signifyingly inhibits CHIKV genome replication. A) Schematic representation of CHIKV *trans*-complementation assay showing codon optimised pCHIKV-nsP1234 (top) from which the CHIKV nsPs were translated and pCHIK-Fluc/Gluc (bottom) in which ORF-1 was replaced by an Fluc reporter gene, fused to the first 77 nts or CHIKV ORF-1 (N77) down stream of the authentic CHIKV 5'UTR. ORF-2, flanked by the authentic intragenic (SG) and 3' UTRs, was replaced by a Gluc reporter gene. **B and C)** Ro significantly inhibited CHIKV genome replication of the *trans*-complementation assay, measured by both ORF-1 and ORF-2 expression, relative to DMSO treated negative controls at 8 and 24 hpt. N=3, error bars represent standard error from the mean and significance was measured by two-tailed T-test (* = $P < 0.05$, ** = $P < 0.01$, *** = $P < 0.001$).
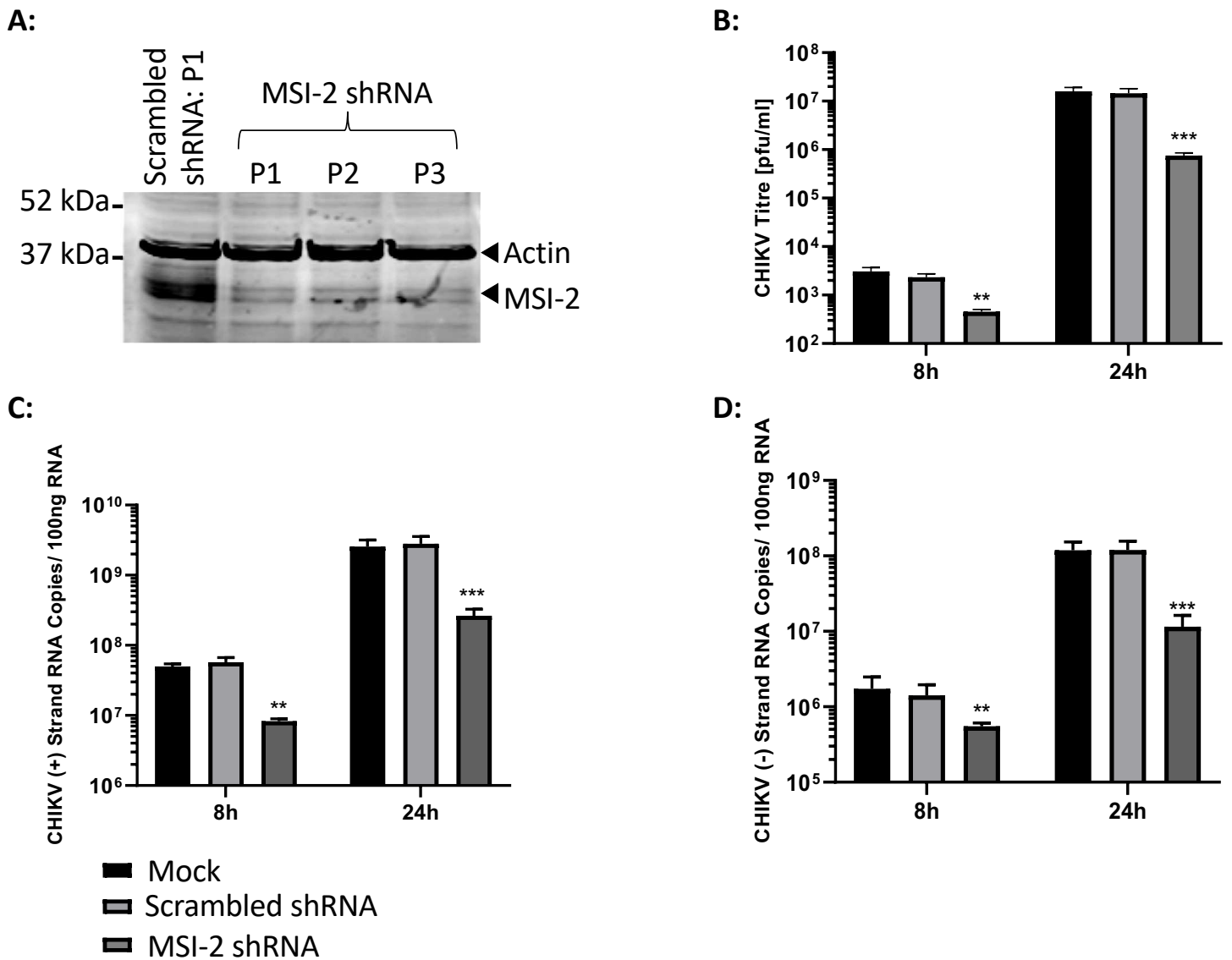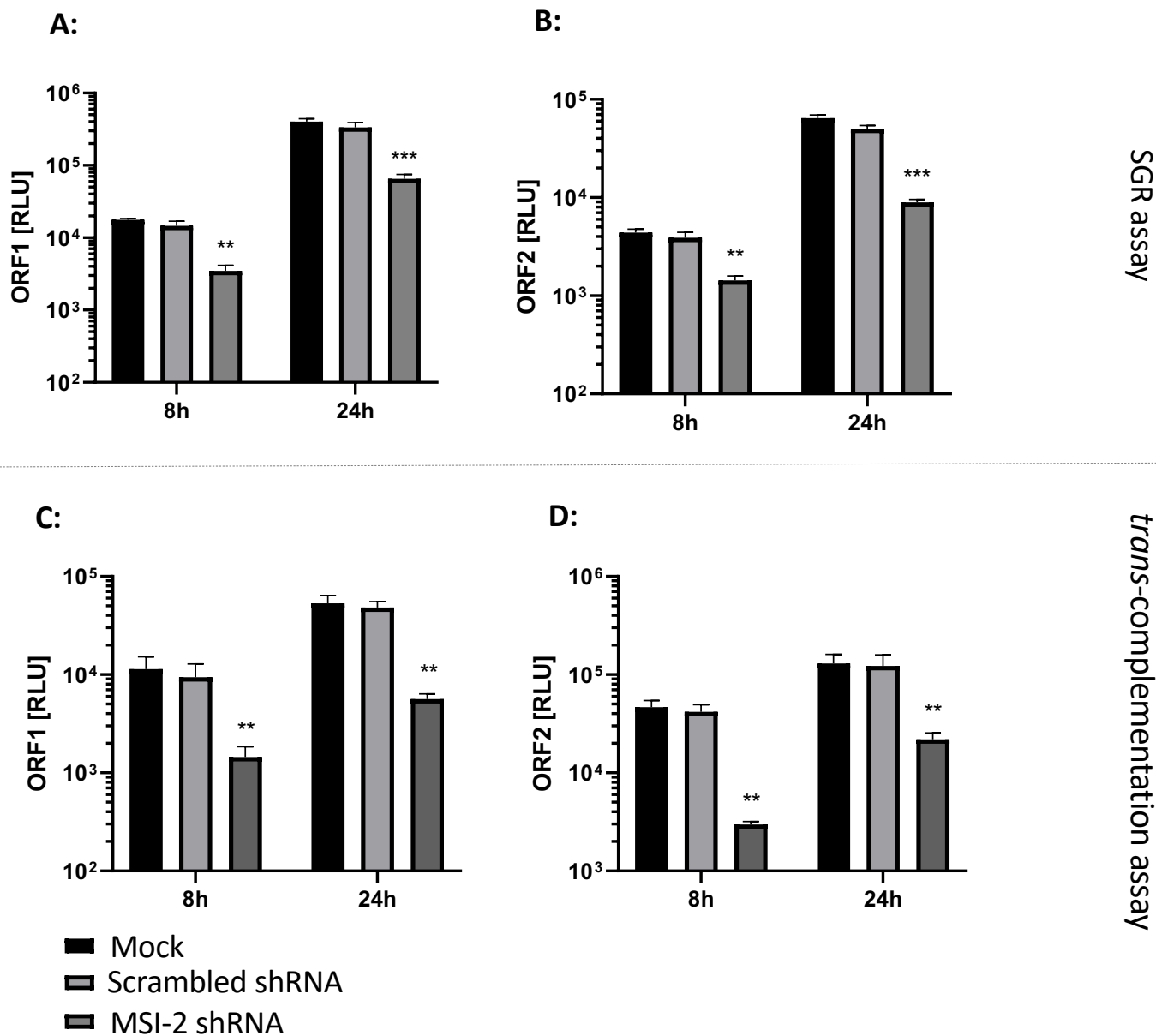
Figure 4. shRNA suppression of MSI-2 significantly inhibits replication of infectious CHIKV. A) Western blot analysis of total cellular protein extracted from Rd cells and compared to negative control scrambled shRNA, demonstrated consistent shRNA knockdown of MSI-2 over 3 serial passages (P1- P3). MSI-2 suppression significantly inhibited productive CHIKV replication, relative to scrambled shRNA at 8 and 24 hpi measured by plaque assay **(B)** and strand specific qRT-PCR for the the virus genomic **(C)** and negative intermediate **(D)** strands. N=3, error bars represent standard error from the mean and significance was measured by two-tailed T-test (* = P < 0.05, ** = P < 0.01, *** = P < 0.001).

Figure 5. shRNA suppression of MSI-2 significantly inhibits CHIKV-SGR replication and CHIKV genome replication. A and **B)** shRNA suppression of MSI-2 significantly inhibited CHIKV-SGR replication, measured by both ORF-1 and ORF-2 expression, relative to scrambled shRNA negative controls at 8 and 24 hpt. **C** and **D**) shRNA suppression of MSI-2 significantly inhibited CHIKV genome replication of the *trans*-complementation assay, measured by both ORF-1 and ORF-2 expression, relative to DMSO treated negative controls at 8 and 24 hpt. N=3, error bars represent standard error from the mean and significance was measured by two-tailed T-test (* = $P < 0.05$, ** = $P < 0.01$, *** = $P < 0.001$).
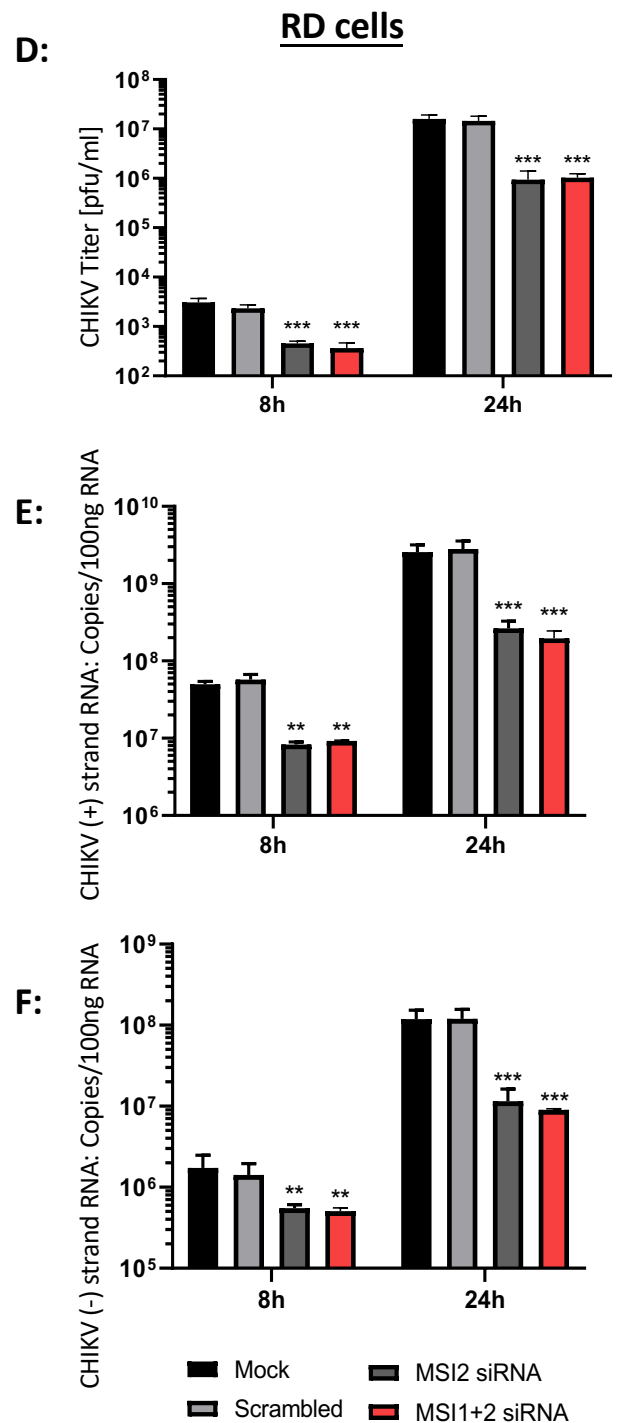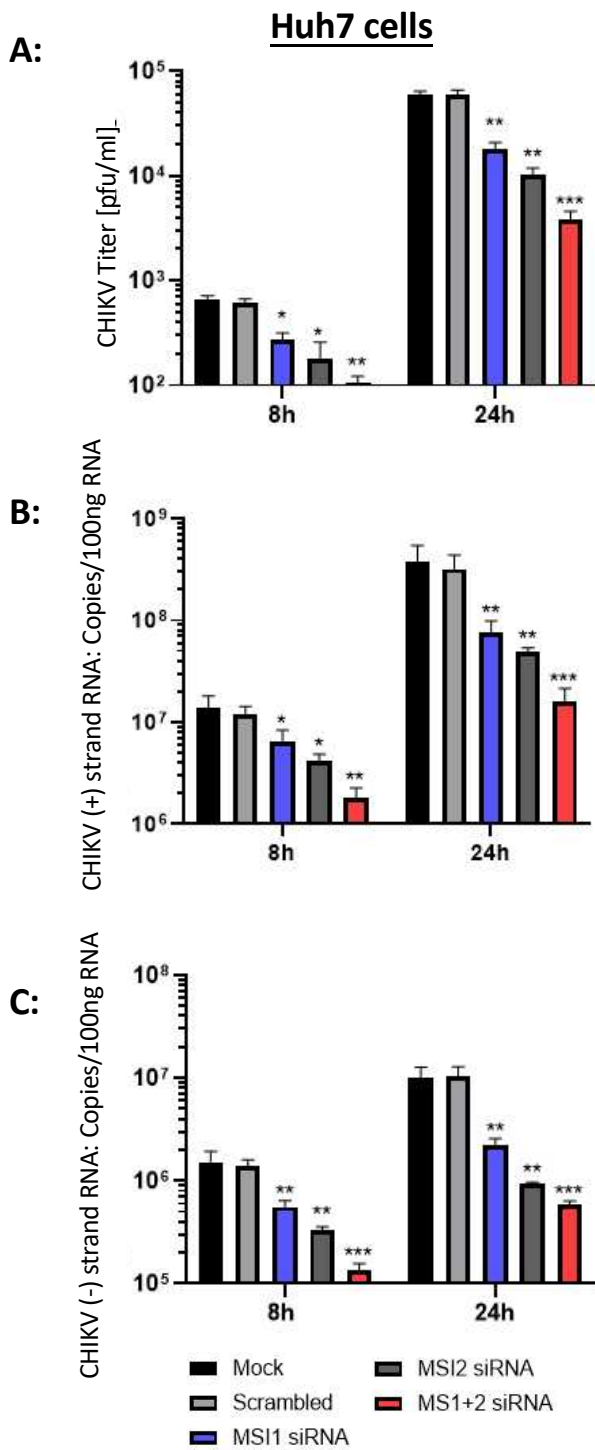
Figure 6: siRNA Depletion of either MSI-1 or MSI-2 significantly inhibited CHIKV replication in Huh7 cells and co-depletion of both MSI-1 and MSI-2 had a synergistic affect on CHIKV inhibition in Huh7 cells. siRNA depletion of MSI-2 significantly inhibited CHIKV replication in RD cells and co-depletion of both MSI-1 and MSI-2 did not increase the level of CHIKV inhibition. siRNA depletion of MSI-1 and MSI-2 significantly inhibited CHIKV replication in Huh7 cells relative to scrambled siRNA at 8 and 24 hpi measured by plaque assay **(A)** and strand specific qRT-PCR for the the virus genomic **(B)** and negative intermediate **(C)** strands. siRNA depletion of MSI-2 in RD cells significantly inhibited CHIKV replication in relative to scrambled siRNA at 8 and 24 hpi measured by plaque assay **(D)** and strand specific qRT-PCR for the the virus genomic **(E)** and negative intermediate **(F)** strands. N=3, error bars represent standard error from the mean and significance was measured by two-tailed T-test (* = P < 0.05, ** = P < 0.01, *** = P < 0.001).
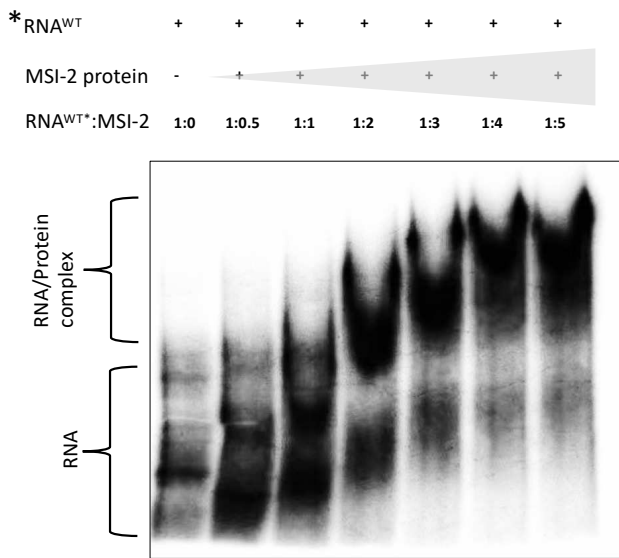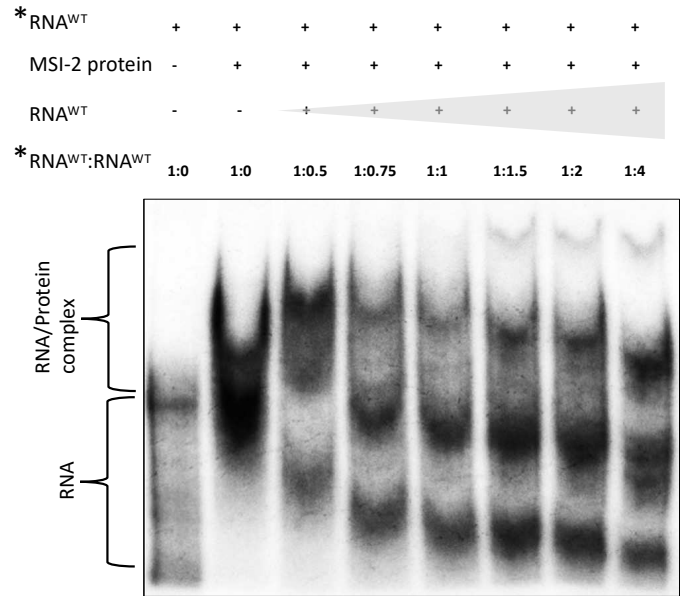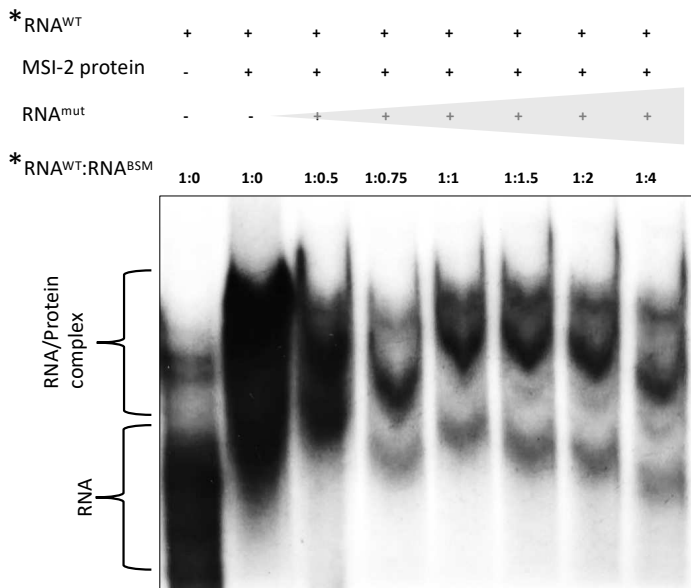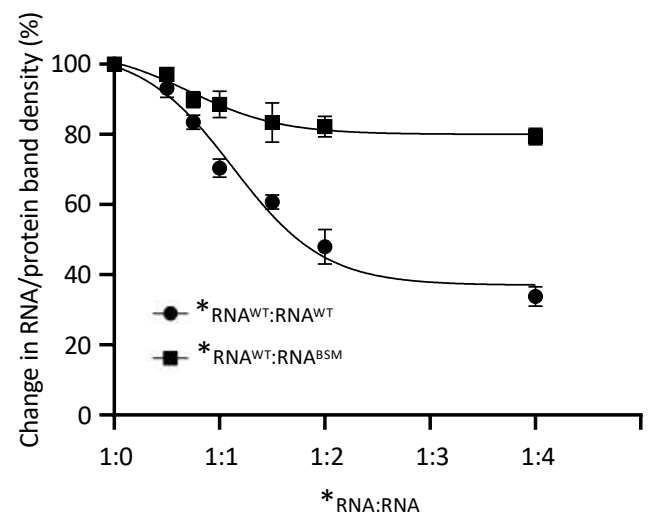
Figure 7. Native EMSAs between *in vitro* transcribed P^{32} 5' radiolabeled CHIKV RNA nts 1-330 (*RNA^{WT}) **and recombinantly expressed MSI-2 demonstrated an RNA/protein interaction that was outcompeted by increasing concentrations of equivalent unlabeled (RNA^{WT}) but less efficiently by the same RNA incorporating BSM mutation $_{63}$AUUAAU$_{68}$ >$_{63}$CAACUU$_{68}$ (RNA^{BSM}). A)** Increasing concentrations of MSI-2 intensified the observed band shift to the larger RNA/Protein complex and decreased the equivalent unbound RNA band. The interaction between a 1:4 ratio of *RNA^{WT}:MSI-2 was competed with increasing concentrations of unlabelled **B)** RNA^{WT} or **C)** RNA^{mut} ($_{63}$CAACUU$_{68}$-mut). **D)** Band shifts in the unlabeled RNA competition EMSAs were quantified by densitometry and expressed as % change in the density of the RNA/Protein complex bands, normalized to the equivalent total lane density, for each competition ratio and compared each time to ratio 1:0. N=3, error bars represent standard error from the mean and significance was measured by two-tailed T-test (* = P < 0.05, ** = P < 0.01, *** = P < 0.001). Grey block triangles indicate increasing concentrations of specific reactants.
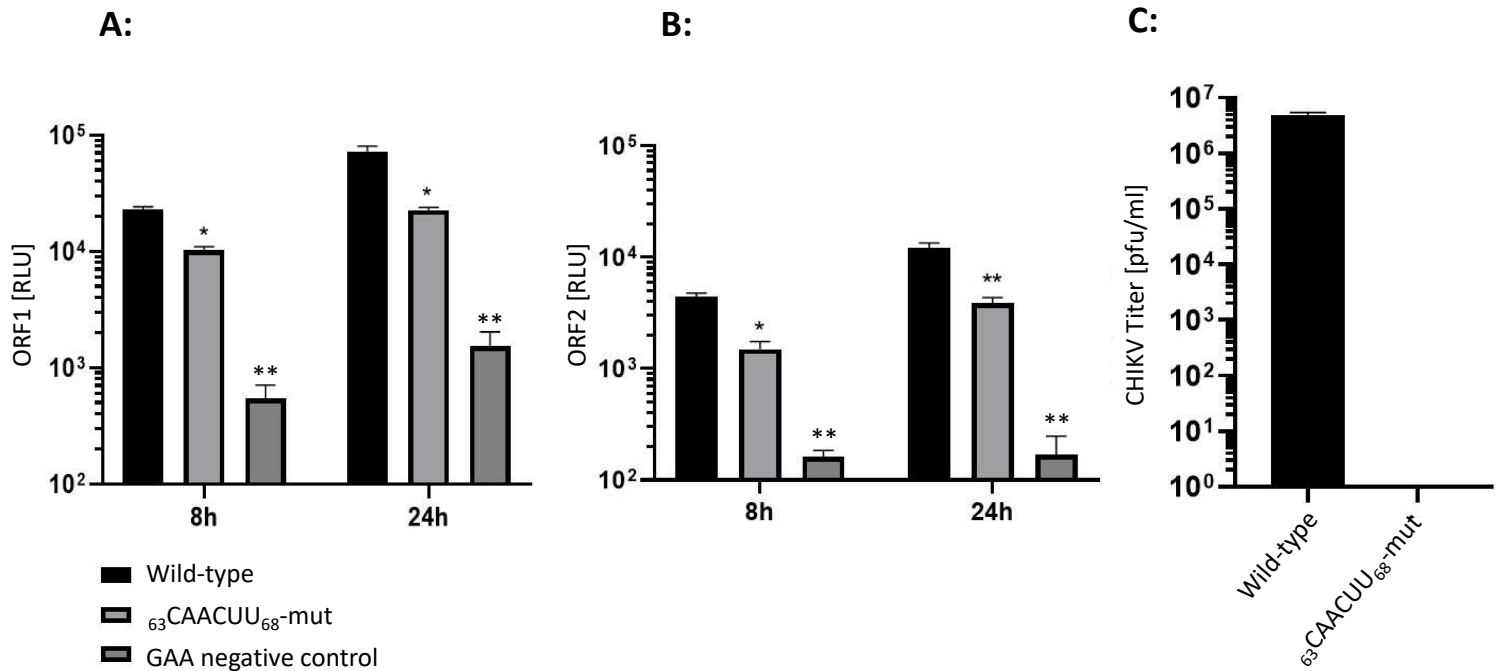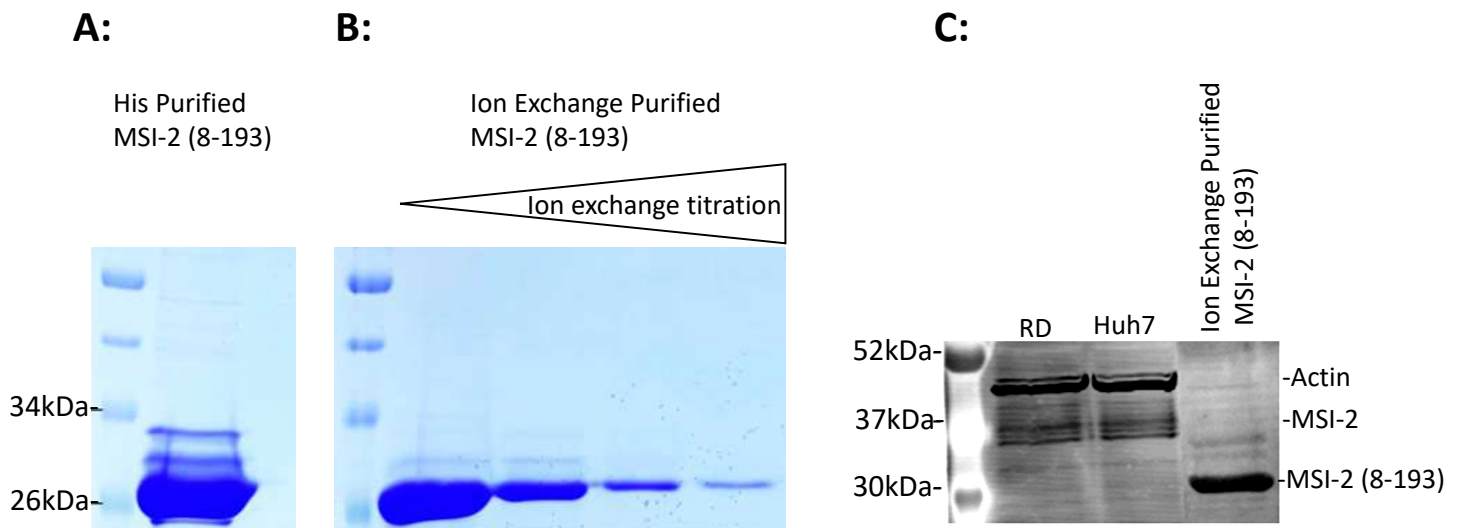
Figure 8. Substitutions within the predicted MSI binding site ($_{63}$CAACUU$_{68}$-mut) prevented rescue of BSM-mutant virus and significantly inhibited CHIKV genome replication. **A and B)** Mutation of the MSI binding site significantly inhibited CHIKV genome replication of the *trans*-complementation assay, measured by both ORF-1 and ORF-2 expression, relative to wild-type positive controls at 8 and 24 hpt. **C)** Mutation of the predicted MSI binding site prevented rescue of BSM-mutant CHIKV following transfection of capped *in vitro* transcribed RNA into BHK cells. Released virus was measured by plaque assay of supernatant 24 hpt and compared to positive control wild-type infectious CHIKV *in vitro* transcribed RNA, which was transfected and analysed in parallel. N=3, error bars represent standard error from the mean and significance was measured by two-tailed T-test (* = P < 0.05, ** = P < 0.01, *** = P < 0.001).

Supplementary data 1: Primers for the reverse transcription and quantitative PCRs for CHIKV strand-specific detection.

CIKV (-) strand detection	PCR	Primer sequence (5'-3')
CHIKV FT tag T	reverse transcription	GGC AGT ATC GTG AAT TCG ATG CGA CAC GGA GAC GCC AAC ATT
Tag T	quantitative	GGC AGT ATC GTG AAT TCG ATG C
CHIKV R T	quantitative	AAT AAA TCA TAA GTC TGC TCT CTG TCT ACA TGA
CHIKV (+) strand detection	PCR	Primer sequence (5'-3')
CHIKV RT tag T	reverse transcription	GGC AGT ATC GTG AAT TCG ATG CGT CTG CTC TCT GTC TAC ATG A
CHIKV F T	quantitative	AAT AAA TCA TAA GAC ACG GAG ACG CCA ACA TT
Tag T	quantitative	see above

Supplementary data 2: Expression and purification of MSI-2 Coomassie stained PAGE analysis following **A)** His Tag and **B)** Ion exchange chromatography. **C)** Ion exchange purified MSI-2 (8-193) analyzed by western blot, relative to total protein extracted from RD and Huh7 cells.

A:

His Purified
MSI-2 (8-193)

34kDa-

26kDa-

B:

Ion Exchange Purified
MSI-2 (8-193)

Ion exchange titration

C:

Ion Exchange Purified
MSI-2 (8-193)

RD   Huh7

52kDa-

37kDa-   -Actin

30kDa-   -MSI-2

                                         -MSI-2 (8-193)

Supplementary data 3: MTT cytotoxicity assay for Ro 08-2750 in RD cells across a titration of 0, 05, 1, 3, 5 10 and 20uM. N=3, error bars represent standard error from the mean.
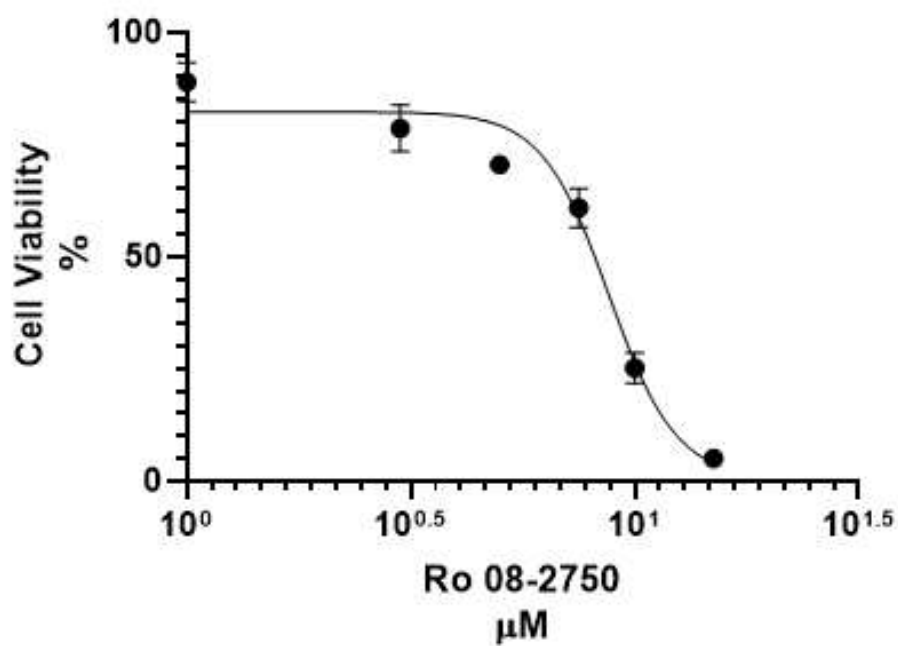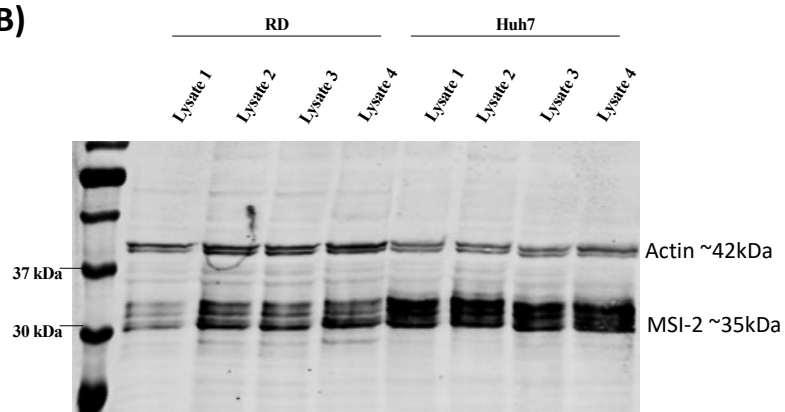
Supplementary data 4: A) MSI-1 and **B)** MSI-2 expression in RD and Huh7 cell lysate analyzed by western blot.
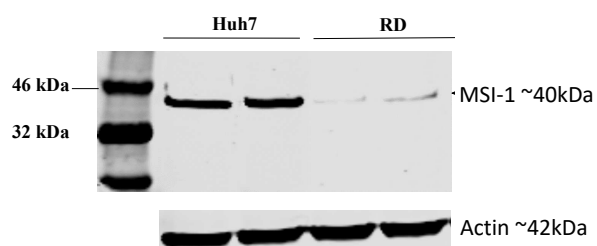
Supplementary data 5: Co-inhibition of MSI-2 and MSI-1 by siRNA in **A)** and **B)** Huh7 cells and **C)** RD cells